International Journal of Scientific Research in Science and Technology
Print ISSN: 2395-6011 | Online ISSN: 2395-602X (www.ijsrst.com)
doi : https://doi.org/10.32628/IJSRST

Segmentation and Detection of Red Blood Cells in Malaria Diagnostic Smears Using U-Net and Yolo V2

Perumallapalli Kavitha[1], Prof. P. Rajesh Kumar[2]
[1]M. Tech (Radar and Microwave Engineering) [1], Andhra University College of Engineering and Technology, Andhra University, Vishakhapatnam, Andhra Pradesh, India
[2]Professor, HOD Electronics and Communication Engineering, Andhra University College of engineering and technology, Andhra University, Vishakhapatnam, Andhra Pradesh, India

Article Info
Volume 9, Issue 5
Page Number : 01-05

Publication Issue
September-October-2022

Article History
Accepted : 20 Aug 2022
Published : 04 Sep 2022

ABSTRACT

Due to their increased precision and reproducibility as compared to manual segmentation and annotation, computer-assisted procedures have become a mainstay of biomedical applications. We present RBC-YOLONet, a novel pipeline for counting and identifying red blood cells in thin blood smear microscopy pictures. It employs a dual deep learning architecture. Two stages make up the RBC-YOLONet: a U-Net first stage for segmenting cell clusters and a YOLOV2 second stage for locating micro cell objects within connected component clusters. To locate tiny objects or fine-scale morphological traits in very large images, RBCNet employs cell clustering, which is robust to cell fragmentation and incredibly scalable. With greater accuracy than traditional and alternative deep learning techniques, the foreground cell-cluster masks from U-Net adaptively direct the detection step in the novel dual cascade RBC-YOLONet architecture. The RBC-YOLONet pipeline is a crucial step in automating malaria diagnosis.

Keywords :- Red blood cells (RBCs), white blood cells (WBCs), deep learning, YOLOV2, connected components, semantic segmentation, U-Net.

I. INTRODUCTION

In the entire world, MALARIA is the number one killer. Mosquito bites are a simple means of transmitting the parasitic infectious disease, which annually causes over 200 million infections and 400 thousand fatalities, with children under five making up the bulk of all malaria-related deaths globally. Sub-Saharan Africa is the area with the highest risk, although half of all people on earth are at risk. The illness starts out with symptoms similar to a cold, such as fever, headache, and chills; however, if left untreated, these symptoms can develop into more serious complications, including kidney failure, anaemia, pulmonary edoema, abnormal liver function, cerebral malaria, neuro-disability, seizures, and ultimately, death. Every year, microscopists check millions of blood smears for the presence of malaria

parasites to establish whether a person is infected or not. This procedure is divided into several steps, beginning with the collection of blood smears, staining of the samples, and examination of the stained slides to identify different cells and spot infected ones. Manual counting and detection requires a microscopist with specialized training and is time-consuming, expensive, and slow. Automated algorithms based on machine learning and image processing offer the potential to provide quick, affordable, and accurate malaria diagnosis while minimizing false positives that frequently occur with manual assessment. Convolutional neural networks have become quite popular recently for tackling problems in machine learning and computer vision since the model learns and computes various properties from the data without any human involvement.

However, these so-called deep learning approaches (DL) require a lot of annotated data as well as computing capacity to acquire the weights necessary to create a predictive model. Because labelled data requires specialized knowledge, getting it is a bottleneck in the medical industry. Developing precise automatic blood cell detection is particularly difficult when it comes to the screening and diagnosis of malaria. Images of various blood smears can differ in terms of staining, resolution, lighting, cell shape, appearance, color, contrast, and debris. Additionally, cells can cluster, making it more difficult to identify individual cells, and staining artefacts can be problematic for image processing techniques that are sensitive. But a number of methods and algorithms have been created with the aim of displacing manual diagnosis, bringing down costs, and accelerating diagnosis.

II. RELATED WORKS

This is a report [1] by WHO malaria report (2019) based on information received from more than 80 countries and areas with ongoing malaria transmission.

This is submission report (2016) of WHO [2] on the final second version of the Malaria microscopy quality assurance manual which was then reviewed by a core group of reviewers, whose inputs were essential.

This is a paper [3] which studies ImageNet deep convolutional neural networks for better use of techniques for preventing overfitting and to improve their performance, that can collect larger datasets and learn more powerful models

This is a study [4] based on previous researches on application of machine learning and now author going for Neural Networks which have many future deep NNs will also take into account that it costs energy to activate neurons, and to send signals between them. Brains seem to minimize such computational costs during problem solving.

This is a survey [5] which have studied nature Deep convolutional nets have brought about breakthroughs in processing images, video, speech and audio

This is basic research [6] which studied the likely lead to larger test suites on patient level, allowing for more standardized evaluations and extensive field testing.

III. METHODOLOGY

U-Net: The U-Net model offers a number of benefits for segmentation tasks. For example, this model enables the simultaneous use of global location and context. Second, it performs better for segmentation tasks even when there are limited training examples available.

UNet, which developed from the conventional convolutional neural network, was initially created and used to process biological images in 2015. While a conventional convolutional neural network focuses on picture classification, where the input is an image and the output is one label, in biomedical situations, it is necessary to not only determine whether a disease exists but also to pinpoint the location of abnormality. UNet is committed to resolving this issue. It can localise and identify borders since every pixel is

classified, ensuring that the input and output are of same size.

It appears to be in the shape of a "U." The design is symmetrical and is divided into two main sections: the left section is known as the contracting path and is made up of the basic convolutional process; the right section is known as the expansive path and is made up of transposed 2D convolutional layers (you can think it as an upsampling technic for now).

YOLOV2: Yolo is quick and effective for processing in the present. Predictions are generated from a single network, including item locations and classes. can be fully taught to increase accuracy. By hovering over a block in YOLOv2, you can get more information about that block. Except for the final convolution block, each convolution block first undergoes BatchNorm normalization before Leaky Relu activation. YOLO creates an SS grid from the input image. Only one object is predicted by each grid cell. In the yellow grid cell below, for instance, an attempt is made to forecast the "person" item whose center (the blue dot) lies within the grid cell. There is a predetermined number of border boxes predicted for each grid cell. In this illustration, the yellow grid cell determines the person's location using two boundary box predictions (blue boxes). The one-object rule does place a limit on how near detected objects can be.

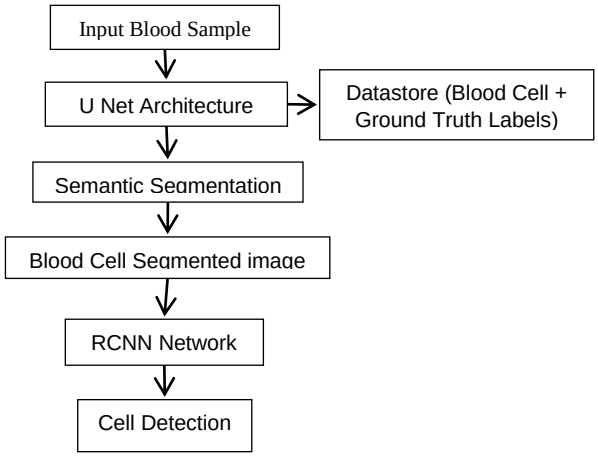

Fig 1: Block Diagram of Proposed Method

For each grid cell,

- Each box has a box confidence score, and it predicts B boundary boxes.
- Regardless of the quantity of boxes B, it only detects one object.
- it detects one object only regardless of the number of boxes B,

It projects probability for the C conditional class (one per class for the likeliness of the object class). Box confidence score is contained in the boundary boxes. The confidence score represents the boundary box's accuracy and the likelihood that the box includes an object (or is objectless). We divide the image's width and height by the bounding box's width and height. The offsets to the relevant cell are x and y. Consequently, all of x, y, w, and h are between 0 and 1. There are 20 conditional class probabilities in each cell. The likelihood that the identified object belongs to a specific class is represented by the conditional class probability (one probability per category for each cell). Each prediction box's class confidence score is calculated as follows:

Class confidence score is equal to box confidence score time's conditional class probability.

It gauges the level of certainty for both the classification and the location (where an object is located). Those score and probability phrases are easy to conflate. For your future reference, listed below are the mathematical definitions

box confidence score $= P_r(object).IoU$

conditional class probability =

$P_r\left(class_i \middle| object\right).IoU$

$class\ confidence\ score = P_r(class_i).IoU$

= box confidence score ×

conditional class probability

Where $P_r(object)$ is the probability, the box contains an object

IoU is the IoU (intersection over union) between the predicted box and the ground truth.

$P_r\left(class_i \mid object\right)$ is the probability the object belongs to $class_i$ given an object is presence.

$P_r(class_i)$ is the probability the object belongs to $class_i$

Multiple bounding boxes are predicted by YOLO for each grid cell. One of them should be in charge of the object in order to calculate the loss for the real positive. For this, we choose the one that has the highest intersection over union (IoU) with the actual data. The forecasts for the bounding box specialise as a result of this tactic. With each forecast, accuracy in predicting specific sizes and aspect ratios increases.

Sum-squared error between the forecasts and the actual data is used by YOLO to determine loss. Assembled into the loss function are:

- The classification loss.
- The localization loss (errors between the predicted boundary box and the ground truth).
- The confidence loss (the objectness of the box).

Classification loss

The classification loss in each cell, provided an object is found, is equal to the squared error of the class conditional probability for each class:

$$\sum_{i=0}^{s^2} \mathbb{1}_i^{obj} \sum_{c \in classes} \left(p_i(c) - \hat{p}_i(c)\right)^2$$

Where

$\mathbb{1}_i^{obj} = 1$ if an object appears in cell *i*, otherwise 0.

$\hat{p}_i(c)$ denotes the conditional class probability for class *c* in cell *i*.

The projected border box sizes and locations are measured by the localization loss. We only include the box that detects the object in our count.

$$\lambda_{coord} \sum_{i=0}^{s^2} \sum_{j=0}^{B} 1_i^{obj} \left[\left(x_i(c) - \hat{x}_i(c)\right)^2 + \left(y_i(c) - \hat{y}_i(c)\right)^2\right] + \lambda_{coord} \sum_{i=0}^{s^2} \sum_{j=0}^{B} 1_i^{obj} \left[\left(\sqrt{x_i} - \sqrt{\hat{x}_i}\right)^2 + \left(\sqrt{h_i} - \sqrt{\hat{h}_i}\right)^2\right]$$

Where $\mathbb{1}_i^{obj} = 1$ if the j th boundary box in cell i is responsible for detecting the object, otherwise 0.

λ_{coord} increase the weight for the loss in the boundary box coordinates.

Absolute errors in large boxes and tiny boxes should not have the same weight. For example, a 2-pixel mistake in a large box has the same effect as one in a tiny one. Yolo forecasts the square root of the width and height of the bounding box rather than the width and height to partially address issue. Additionally, we double the loss by λcoord to place a greater focus on the border box precision (default: 5).

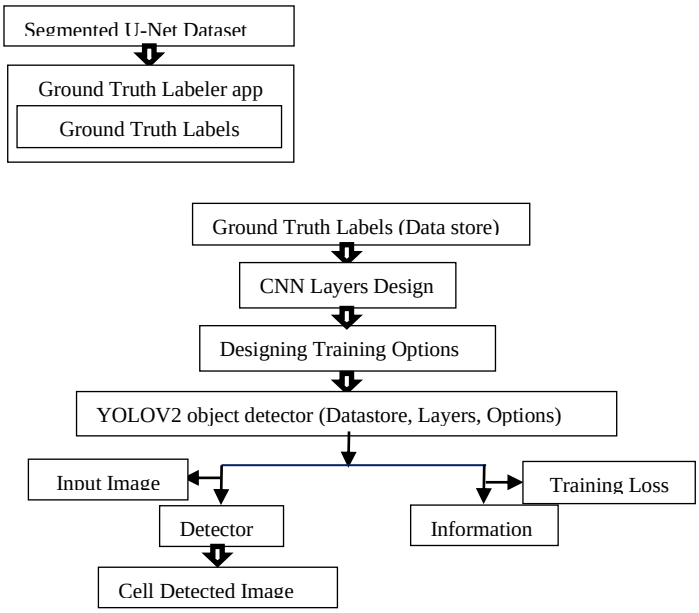

Fig 2: Yolo V2 Architecture

IV. EXPERIMENTAL RESULTS

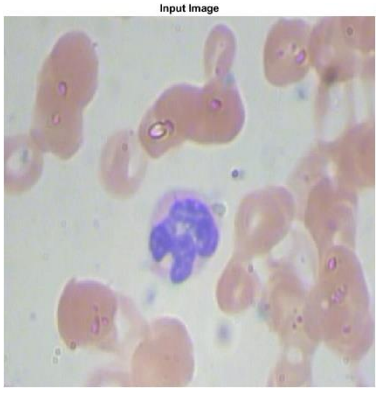

Fig 3: Input Image

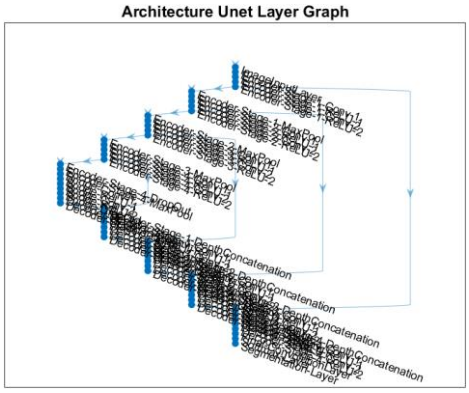

Fig 4: Architecture U Net Layer Graph

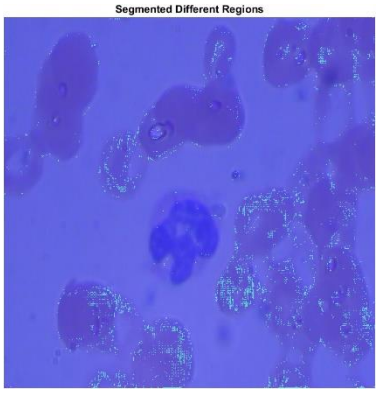

Fig 5: Segmented Different Regions

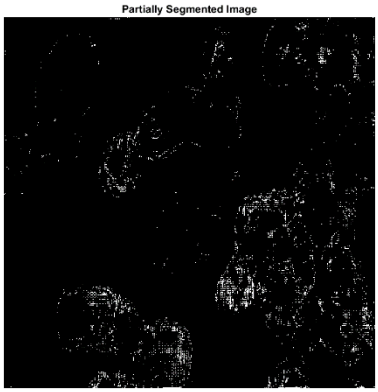

Fig 6: Partially Segmented Image

Fig 7: Final Segmented Image

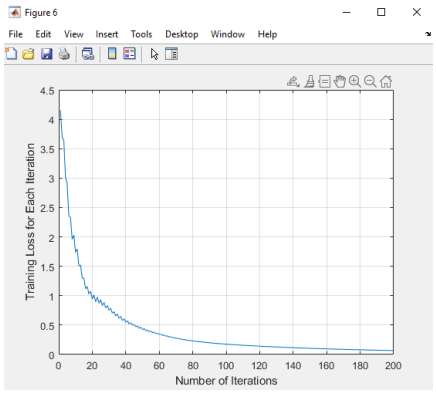

Fig 8: Training Loss

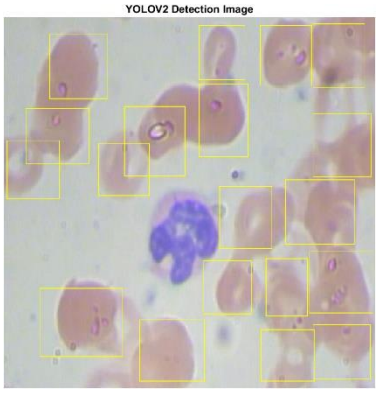

Fig 9: YOLOV2 Detection Image

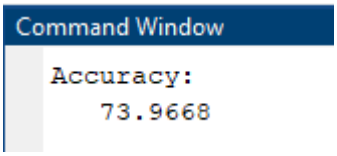

Fig 10: Command window results

S. No	Existing Method	Proposed Method
1	56.51	84.51
2	68.92	97.92
3	75.26	90.26
4	56.25	80.25
5	54.96	73.96

Fig 11: Accuracy Comparison Table

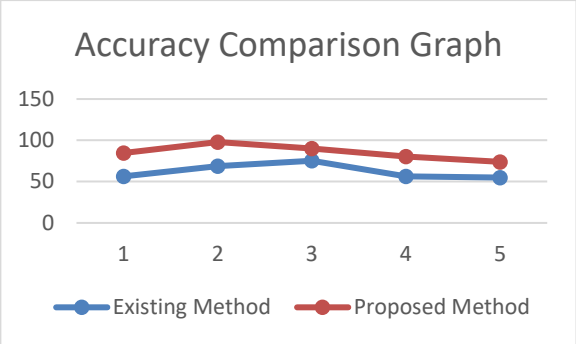

Fig 12: Accuracy Comparison Graph

V. CONCLUSION

The RBC-YOLONet pipeline uses a dual deep learning architecture to identify and count red blood cells in thin blood smear microscopy images. The RBC-YOLONet system consists of two stages: a U-Net first stage for segmenting cell-clusters and a YOLOV2 second stage for finding small cell objects within connected component clusters. RBCNet is highly scalable and resistant to cell fragmentation since it recognizes small items or fine scale morphological traits in very large images using cell clustering rather than region recommendations. An essential stage in automating malaria detection is the RBC-YOLONet pipeline. Other two-stage deep learning object detectors, such as ones that make use of convolutional neural networks (Faster R-CNNs) in some locations, are slower than YOLO v2. In contrast to conventional and other deep learning systems, the ground-breaking dual cascade RBC-YOLONet architecture enables more precise cell detections since the foreground cell-cluster masks from U-Net adaptively direct the identification step.

VI. REFERENCES

[1]. WHO, "World malaria report 2019," World Health Organization, Geneva, Switzerland, Rep. 2019, 2019.

[2]. WHO, "Malaria microscopy quality assurance manual-version 2," World Health Organization, Geneva, Switzerland, Rep. no. 2016, 2016.

[3]. A. Krizhevsky, I. Sutskever, and G. E Hinton, "Imagenet classification with deep convolutional neural networks," in Proc. Adv. Neural Inf. Process. Syst., 2012, pp. 1097–1105.

[4]. J. Schmidhuber, "Deep learning in neural networks: An overview," Neural Netw., vol. 61, pp. 85–117, 2015.

[5]. Y. LeCun, Y. Bengio, and G. Hinton, "Deep learning," Nature, vol. 521, no. 7553, pp. 436–444, 2015. 1746 IEEE JOURNAL OF BIOMEDICAL AND HEALTH INFORMATICS, VOL. 25, NO. 5, MAY 2021.

[6]. M. Poostchi, K. Silamut, R. J. Maude, S. Jaeger, and G. Thoma, "Image analysis and machine learning for detecting malaria," Transl. Res., vol. 194, pp. 36–55, 2018.patients with 2019 novel coronavirus–infected pneumonia inWuhan, China." Jama (2020).

[7]. D. Anggraini, A. S. Nugroho, C. Pratama, I. E. Rozi, V. Pragesjvara, and M. Gunawan, "Automated status identification of microscopic images obtained from malaria thin blood smears using bayes decision: A study case in plasmodium falciparum," in Proc. Int. Conf. Adv. Comput. Sci. Inf. Syst., Dec. 2011, pp. 347–352.

[8]. L. Malihi, K. Ansari-Asl, and A. Behbahani, "Malaria parasite detection in giemsa-stained blood cell images," in Proc. Iranian Conf. Mach. Vis. Image Process., Sep. 2013, pp. 360–365.

[9]. S. S. Savkare and S. P. Narote, "Automated system for malaria parasite identification," in Proc. Int. Conf. Commun., Inf. Comput. Technol., Jan. 2015, pp. 1–4.

[10]. S. S. Devi, A. Roy, M. Sharma, and R. H. Laskar, "knnNN classification-based erythrocyte separation in microscopic images of thin blood smear," in Proc. Int. Conf. Comput. Intell. Netw., Jan. 2016, pp. 69–72.

[11]. N. Abbas et al., "Microscopic rgb color images enhancement for blood cells segmentation in ycbcr color space for k-means clustering," J.

Theor. Appl. Inf. Technol., vol. 55, no. 1, pp. 117–125, 2013.

[12]. A. S. Abdul-Nasir, M. Y. Mashor, and Z. Mohamed, “Colour image segmentation approach for detection of malaria parasites using variouscolour models and k-means clustering,” WSEAS Trans. Biol. Biomed., vol. 10, no. 1, pp. 41–55, 2013.

Cite this article as :

Perumallapalli Kavitha, Prof. P. Rajesh Kumar, "Segmentation and Detection of Red Blood Cells in Malaria Diagnostic Smears Using U-Net and Yolo V2", International Journal of Scientific Research in Science and Technology (IJSRST), Online ISSN : 2395-602X, Print ISSN : 2395-6011, Volume 9 Issue 5, pp. 01-07, September-October 2022.
Journal URL : https://ijsrst.com/IJSRST2294125